A Complete Hysterical Constitutive Law for Reinforced Concrete under Earthquake Loadings

H.H. Lavassani[1], A.A. Tasnimi[2*], and M. Soltani M. [3]

1. Ph.D. Student, Dept. of Civil Engineering, School of Engineering, Tarbiat Modares Univ., Tehran, Iran
2. Prof., Dept. of Civil Engineering, School of Engineering, Tarbiat Modares Univ., Tehran, Iran
* Corresponding Author: email: tasnimi@modares.ac.ir
3. Assistant Prof., Department of Civil Engineering, School of Engineering, Tarbiat Modares Univ., Tehran, Iran

ABSTRACT

A hysterical constitutive law for reinforced concrete subjected to earthquake loadings in both compression and tension is presented in this study. This constitutive law is selected to provide improvements on modeling the hysterical behavior of concrete structures in the finite element codes under earthquake loadings. The fundamental framework of the presented concept is the stress-based elasto-plastic-damage-fracture (EPFD) theory. In this theory applied relationships in compression domain include the elasto-plastic-damage behavior and in tension domain, include the elasto-plastic-fracture behavior. The main novelty of the proposed hysterical constitutive law for reinforced concrete lies in the fact that the foundation of constitutive formulations are based on thermodynamics framework and all the required parameters can be obtained through simple formal tests. In the case of earthquake loading, the 1/3 scaled wall model, which was tested on the shaking table at C.E.A., has been derived from experimental results obtained by considering the dependency of the hysterical parameters with the EPFD attained by the concrete.

Keywords:
Elasto-plastic-damage-fracture; Hysterical constitutive Law; Potential function; Reinforced concrete; Earthquake loading

1. Introduction

The rational computational analysis of reinforced concrete structures subjected to earthquake loadings requires realistic mathematical description of the material response under various stresses. The requirements characterize *RC* behavior with a constitutive law, which gives the stress as a function of strain, for reproducing the exact behavior of the structures. In order to model the behavior of concrete structures under earthquake loading, it is essential to model the tension and compression envelope curves and properties of the concrete material.

In this paper, a novel *EPFD* constitutive law for predicting the cyclic parameters of reinforced concrete and damage of concrete subjected to earthquake loading is presented.

In the past, different constitutive laws have been presented to realize the behavior of concrete in many articles [1-15]. Numerous concrete models have been proposed in the recent years. In the macroscopic level, four broad categories can be distinguished: a) models derived from the theory of elasticity, b) models based on the theory of plasticity [4, 11, 16], c) models based on the continuum damage theory [7, 15, 17, 18, 19], and d) models based on the fracture mechanics [1, 9, 10, 12, 18, 20, 21, 22]. Also, some coupled models based on the association of elasto-plasticity and continuum damage theory [3, 5, 6, 13, 14, 23], and elasto-plasticity and fracture mechanics [13], have been recently developed.

The first objective of the present study is to find a novel general potential function which can estimate the behavior of materials in different conditions due to variation of material parameters. This potential function should satisfy a complete description of the elastic compression strains, the elastic tension strains, the plastic compression strains, the micro cracks in tensions, the micro crashes in compression, the cracks in tension, and the crashes in compression.

The constitutive law created by this novel potential function could describe the behavior of concrete for unconfined and confined state under earthquake loadings.

In this study, a complete uniaxial hysterical constitutive law is presented for reinforced concrete. For this constitutive law, mechanical formulations were derived from the thermodynamic principles and were verified by generalization of test results for concrete under cyclic and earthquake loading histories. Many uniaxial stress-strain models have been documented by different researchers, such as [24-27]. Most of them refer only to the compressive cyclic behavior of concrete and just a few consider the cyclic tension response.

This paper is organized as the following. First, the theory of constitutive law of reinforced concrete based on thermodynamics framework will be introduced. In the next section, the mapping of the complete hysterical constitutive law based on *EPFD* theory will be presented. The *F.E.M.* relations required for modeling of reinforced concrete structure under earthquake loading will be then rewritten in steady state. And finally, the law will be verified, a numerical study for simple cases will be presented, and some conclusions will be presented.

2. The Constitutive Law Governing Reinforced Concrete

In this section, a framework for deriving novel constitutive law provided by thermodynamics is established. In the first step, the terminology of classical thermodynamics is used, but some minor changes are convenient. The classical thermodynamics makes use of the intensive quantities pressure p and temperature Q, together with extensive quantities specific[1] volume v, and specific entropy s. Four energy functions are defined, the specific internal energy, specific Helmholtz free energy, specific enthalpy and specific Gibbs free energy. Each energy function is defined by two state variables, and other state variables are obtained by the differentials. The Helmholtz free energy is a Legendre transform of the internal energy, in which the roles of entropy and specific volume are interchanged. In this paper, the relations are expanded based on Helmholtz free energy. In applying thermodynamics to quasi brittle materials as concrete, it is necessary to replace the role of pressure by the stress tensor, and the specific volume by the strain tensor. Therefore, The Helmholtz free energy may be expressed in the form of $Y_f(\varepsilon_{ij}, Q)$, and the following relationships are then readily obtained as $\sigma_{ij} = \rho_0 \dfrac{\partial Y_f}{\partial \varepsilon_{ij}}$, and $s = \rho_0 \dfrac{\partial Y_f}{\partial Q}$.

2.1. First Law of Thermodynamics

After this introductory description, the first law of thermodynamics can now be presented in a general form suitable for purposed constitutive law of reinforced concrete. In global form, the first Law of Thermodynamics is $\dot{E}_k + \dot{Y}_u = \dfrac{\delta W}{dt} + \dfrac{\delta Q}{dt}$. Where, $\dot{E}_k, +\dot{Y}_u, W$, and Q are the rate of kinetic energy, the rate of potential energy, the mechanical work input, and the heat supply to an element of volume respectively. Since this expression holds for arbitrary regions volume, the local form of first law is $\rho_0 \dot{Y}_u = \dot{\varepsilon}_{ij}\sigma_{ij} + r_h + q_{i,j}$, where r_h and q_i denote the amount of heat supply per unit time and unit volume and heat flux vector respectively. The local form of the first law of thermodynamics holds at every point in body. Now, considering the concept of thermodynamic state of the material, internal kinematic variables as well as the extensive quantities must be presented. In *EPFD* theory, for convenience some kinematic internal variables of tonsorial forms shall be considered. The Helmholtz free energy now takes the form $Y_f(\varepsilon_{ij}, Q, \kappa_{ij}^{pl}, \kappa_{ij}^{fr}, \kappa_{ij}^{da})$.

2.2. Clausius-Duhem Inequality

The second law of thermodynamics in this case still cast in its local form is $\rho_0 Q\dot{s} + q_{i,i} - \dfrac{q_i Q_{,i}}{Q} \geq 0$. The dissipation here comprises two parts corresponding to the mechanical dissipation $\rho_0 Q\dot{s} + q_{i,i}$ and thermal dissipation $(-\dfrac{q_i Q_{,i}}{Q})$. As mentioned in the original frame work [28-29], a more stringent law than the second law of thermodynamics can be assumed here by presuming that $\rho_0 Q\dot{s} + q_{i,i} \geq 0$, using the fact that the thermal dissipation is always non-negative and small, compared to the mechanical dissipation for small thermal gradients. Therefore the dissipation function, which is actually the rate of dissipation, corresponding to Helmholtz free energy, is $d_{mech}^f = \rho_0\sigma_{ij}\dot{\varepsilon}_{ij} - \rho_0\dot{Y}_f - \rho_0 Q\dot{s}$. Therefore, the Clausius-Duhem inequality is obtained. In elasto-plastic-fracture and damage theory, the dissipation of Helmholtz free energy takes the form of $d_{mech}^f(\varepsilon_{ij}, Q, \kappa_{ij}^{pl}, \kappa_{ij}^{fr}, \kappa_{ij}^{da}, \varepsilon_{ij}^{pl}, \varepsilon_{ij}^{fr}, \varepsilon_{ij}^{da})$.

1. The specific quantities are each defined as per unit mass.

2.3. The Choice of Evolution Laws Fulfillment of the EPFD Mechanical Dissipation Inequality

The *EPFD* constitutive law must fulfill the mechanical dissipation inequality. The *EPFD* mechanical dissipation inequality appears from section (2.2) as:

$$d^f_{mech} = \rho_0 \sum_{e=}^{pl,fr,da} \left(\frac{\partial Y_f}{\partial \dot{\kappa}^e_{ij}} \dot{\kappa}^e_{ij} - \frac{\partial Y_f}{\partial \varepsilon_{ij}} \dot{\varepsilon}^e_{ij} \right) + \rho_0 \frac{\partial Y_f}{\partial \varepsilon_{ij}} \dot{\varepsilon}_{ij} + \rho_0 \frac{\partial Y_f}{\partial Q} \dot{Q} - \dot{Y}_f \geq 0 \quad (1)$$

In this equation, $\dot{\kappa}^{pl}_{ij}, \dot{\kappa}^{da}_{ij}, \dot{\kappa}^{fr}_{ij}, \dot{\varepsilon}^{pl}_{ij}, \dot{\varepsilon}^{da}_{ij}$, and $\dot{\varepsilon}^{fr}_{ij}$ are the flaxes in a way that the *EPFD* mechanical dissipation of Helmholtz free energy is fulfilled. In the following according to *EPFD* evolution laws, $\dot{\kappa}^{pl}_{ij}, \dot{\kappa}^{da}_{ij}, \dot{\kappa}^{fr}_{ij}, \dot{\varepsilon}^{pl}_{ij}, \dot{\varepsilon}^{da}_{ij}$, and $\dot{\varepsilon}^{fr}_{ij}$ are determined, and a complete way to establish such *EPFD* evolution laws are provided. The *EPFD* mechanical dissipation of Helmholtz free energy can be written in a simple form. Like other evolution laws, the sets *EPFD* conjugated thermodynamics forces A_κ and *EPFD* fluxes $\dot{a}_\kappa$ are defined for this propose by:

$$A_\kappa = \left\{ \frac{\partial Y_f}{\partial \kappa^{pl}_{ij}}, \frac{\partial Y_f}{\partial \kappa^{da}_{ij}}, \frac{\partial Y_f}{\partial \kappa^{fr}_{ij}}, \frac{\partial Y_f}{\partial \varepsilon^{pl}_{ij}}, \frac{\partial Y_f}{\partial \varepsilon^{da}_{ij}}, \frac{\partial Y_f}{\partial \varepsilon^{fr}_{ij}} \right\}$$
$$\dot{a}_\kappa = \left\{ \dot{\kappa}^{pl}_{ij}, \dot{\kappa}^{da}_{ij}, \dot{\kappa}^{fr}_{ij}, \dot{\varepsilon}^{pl}_{ij}, \dot{\varepsilon}^{da}_{ij}, \dot{\varepsilon}^{fr}_{ij} \right\} \quad (2)$$

So, the *EPFD* mechanical dissipation of Helmholtz free energy is changed to $d^f_{mech} = A_\kappa \dot{a}_\kappa \geq 0$. If all forces are zero, it seems reasonable to assume that also all fluxes are zero (if $A_\kappa = 0$ then $\dot{a}_\kappa = 0$). In this paper, the potential approach is applied for establishment of the *EPFD* evolution laws for $\dot{a}_\kappa$ so that the *EPFD* mechanical dissipation of Helmholtz free energy is fulfilled (For more information, see Appendix (I), and Figure (1)).

2.4. Yield Surface

For a rate-independent material (like concrete) the dissipation must be a homogeneous first order function in $\dot{a}_\kappa$, since (for fixed ratios between the rates) the magnitude of dissipated energy must be directly proportional to the magnitude of deformation. For a homogeneous first order function, Euler's theorem gives:

$$d^f_{mech} = \frac{\partial d^f_{mech}}{\partial \dot{a}_\kappa} \dot{a}_\kappa = \overline{A}_\kappa \dot{a}_\kappa \quad (3)$$

And comparing $\overline{A}_\kappa \dot{a}_\kappa$ with $A_\kappa \dot{a}_\kappa$, the following

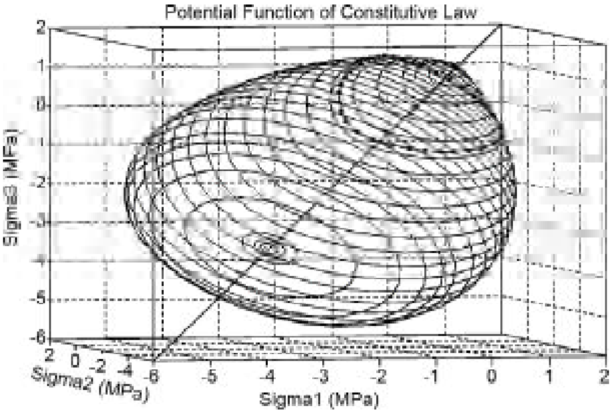

Figure 1. The generation of F_{pl} function of concrete.

is obtained:

$$(\overline{A}_\kappa - A_\kappa)\dot{a}_\kappa = 0 \quad (4)$$

The roles of the *EPFD* fluxes $\dot{a}_\kappa$ and the sets of conjugated dissipation forces $\overline{A}_\kappa$ can now be interchanged by a further Legendre transform. The transform of the dissipation function is in fact the yield function $y^f(\varepsilon_{ij}, \dot{a}_\kappa, \overline{A}_\kappa, Q)$, and can be written as:

$$\lambda^y y^f = d^f_{mech} - A_\kappa \dot{a}_\kappa = 0 \quad (5)$$

The differential of the yield function gives the flow rule $(\dot{a}_\kappa = \lambda^y \frac{\partial y^f}{\partial \overline{A}_\kappa})$. The consistency conditions can be then used to evaluate the change of the plastic, damage and fracturing multipliers.

$$\begin{cases} \dot{y}^f_{pl} = \dfrac{\partial y^f_{pl}}{\partial A^{pl}_k} A^{pl}_k + H^{pl}.\dot{\lambda}^y_{pl} = 0 \\ \dot{y}^f_{fr} = \dfrac{\partial y^f_{fr}}{\partial A^{fr}_k} A^{fr}_k + H^{fr}.\dot{\lambda}^y_{fr} = 0 \\ \dot{y}^f_{da} = \dfrac{\partial y^f_{da}}{\partial A^{da}_k} A^{da}_k + H^{da}.\dot{\lambda}^y_{da} = 0 \end{cases} \quad (6)$$

2.5. Generating an EPFD Constitutive Law

Adopting the approach described above, the *EPFD* constitutive law of reinforced concrete is entirely defined by the specification of two potentials:

a) The Helmholtz free energy potential.
b) The yield surface.

Therefore, the principle *EPFD* constitutive laws are obtained as follows:

$$\begin{cases} \sigma_{ij} = \dfrac{\partial Y_f}{\partial \varepsilon_{ij}} \\ s = \dfrac{\partial Y_f}{\partial Q} \end{cases}, \begin{cases} A_\kappa = \dfrac{\partial Y_f}{\partial a_\kappa} \\ \dot{a}_\kappa = \lambda^y \dfrac{\partial y^f}{\partial \overline{A}_\kappa} \end{cases} \quad (7)$$

In the numerical analysis of problems involving nonlinear materials under earthquake loading, the incremental form of the *EPFD* constitutive law is usually required. This, for instance, often forms a central part of a finite element analysis.

$$\begin{Bmatrix} \dot{\sigma}_{ij} \\ \dot{A}_k \\ -\dot{s} \end{Bmatrix} = \begin{bmatrix} \frac{\partial^2 Y_f}{\partial\dot{\varepsilon}_{ij}\partial\dot{\varepsilon}_{ij}} & \frac{\partial^2 Y_f}{\partial\dot{\varepsilon}_{ij}\partial a_k} & \frac{\partial^2 Y_f}{\partial\dot{\varepsilon}_{ij}\partial Q_{ij}} \\ \frac{\partial^2 Y_f}{\partial a_k\partial\dot{\varepsilon}_{ij}} & \frac{\partial^2 Y_f}{\partial a_k\partial a_k} & \frac{\partial^2 Y_f}{\partial\dot{\varepsilon}_{ij}\partial Q} \\ \frac{\partial^2 Y_f}{\partial\dot{\varepsilon}_{ij}\partial Q} & \frac{\partial^2 Y_f}{\partial a_k\partial Q} & \frac{\partial^2 Y_f}{\partial Q\partial Q} \end{bmatrix} \begin{Bmatrix} \dot{\varepsilon}_{ij} \\ \dot{a}_k \\ \dot{Q} \end{Bmatrix} \quad (8)$$

For the plastic multiplier $\dot{\lambda}^y_{pl}$, the following are satisfied:

$$\begin{cases} F_{pl} = 0 \xrightarrow{\dot{\lambda}^y_{pl}=0} neutral\ loading \\ F_{pl} = 0 \xrightarrow{\dot{\lambda}^y_{pl}>0} plastic\ loading \\ F_{pl} < 0 \xrightarrow{\dot{\lambda}^y_{pl}=0} elastic\ loading \end{cases} \quad (9)$$

And the plastic consistency condition is $\dot{\lambda}^y_{pl}\dot{F}_{pl} = 0$. It is assumed that the strain is divided into elastic, plastic, damage and fracture strains.

$$\varepsilon = \varepsilon^{el} + \varepsilon^{pl} + \varepsilon^{da} + \varepsilon^{fr} \quad (10)$$

And the Helmholtz free energy is divided into four parts:

$$Y_f = Y_f^{el}(\varepsilon^{el}) + Y_f^{pl}(A_k^{pl}) + Y_f^{da}(\varepsilon^{da}, A_k^{da}) + Y_f^{fr}(\varepsilon^{fr}, A_k^{fr}) \quad (11)$$

$$d^f_{mech} = d^{el} + d^{pl} + d^{fr} + d^{da} \geq 0 \quad (12)$$

Where:

$$\begin{cases} d^{el} = \left(\sigma - \frac{\partial Y_f^{el}}{\partial\varepsilon^{el}}\right) : \dot{\varepsilon}^{el} \geq 0 \\ d^{pl} = \sigma : \dot{\varepsilon}^{pl} - \frac{\partial Y_f^{pl}}{\partial a_k^{pl}}\dot{a}_k^{pl} \geq 0 \\ d^{da} = \sigma : \dot{\varepsilon}^{da} - \frac{\partial Y_f^{da}}{\partial a_k^{da}}\dot{a}_k^{da} \geq 0 \\ d^{fr} = \sigma : \dot{\varepsilon}^{fr} - \frac{\partial Y_f^{fr}}{\partial a_k^{fr}}\dot{a}_k^{fr} \geq 0 \end{cases}$$

To better identify the *EPFD* response introduced by the considerations presented in the previous sections by the total stress-strain relations, in this section, the tangent rate equations, associated to the general laws developed above are derived. Global relations between the rates of total strain $\dot{\sigma}$ and stress are obtained as follows. The rate form of the elastic relation leads to:

$$\dot{\sigma} = E^{el}\dot{\varepsilon}^{el} = E^{el}(\dot{\varepsilon} - \dot{\varepsilon}^{pl} - \dot{\varepsilon}^{fr} - \dot{\varepsilon}^{da}) \quad (13)$$

where, $E^{el} = \frac{\partial^2 Y_f^{el}}{\partial(\varepsilon^{el})^2}$. The fracture strain rates $\dot{\varepsilon}^{fr}$ in this last expression are eliminated in the usual way. Indeed, the imposition of the fracture consistency in combination with Eq. (13) leads to:

$$\dot{\sigma} - E^{el}\dot{\varepsilon}^{fr} = E^{el}(\dot{\varepsilon} - \dot{\varepsilon}^{pl} - \dot{\varepsilon}^{da}) \quad (14)$$

$$\dot{\sigma} = \left(2I \underline{\otimes} I - E^{el}E^{fr\text{-}1}\right)^{-1} E^{el}(\dot{\varepsilon} - \dot{\varepsilon}^{pl} - \dot{\varepsilon}^{da}) \quad (15)$$

We arrive at the tangent relation $E^{ef} = (2I \underline{\otimes} I - E^{el}E^{fr^{-1}})^{-1}E^{el}$.

$$\dot{\sigma} = E^{ef}(\dot{\varepsilon} - \dot{\varepsilon}^{pl} - \dot{\varepsilon}^{da}) \quad (16)$$

The plastic strain rates $\dot{\varepsilon}^{pl}$ in this last expression are eliminated in the usual way. Indeed, the imposition of the plastic consistency in combination with Eq. (16) leads to:

$$\dot{\sigma} - E^{ef}\dot{\varepsilon}^{pl} = E^{el}(\dot{\varepsilon} - \dot{\varepsilon}^{da}) \quad (17)$$

We arrive at the *EPFD* tangent relation $E^{epf} = E^{ef} -$

$$\frac{E^{ef}\frac{\partial F_{pl}}{\partial\sigma} \otimes \frac{\partial F_{pl}}{\partial\sigma}E^{ef}}{\left(\frac{\partial F_{pl}}{\partial A_k^{pl}}\right)^2 \frac{\partial^2 Y_f^{pl}}{\partial a_k^2} + \frac{\partial F_{pl}}{\partial\sigma} : E^{ef} : \frac{\partial F_{pl}}{\partial\sigma}}.$$

$$\dot{\sigma} = E^{epf}(\dot{\varepsilon} - \dot{\varepsilon}^{da}) \quad (18)$$

Finally, the damage strain rates $\dot{\varepsilon}^{da}$ in this last expression are eliminated in the usual way. Indeed, the imposition of the plastic consistency in combination with Eq. (18) leads to:

$$\dot{\sigma} = E^{epf}\dot{\varepsilon}^{da} = E^{epf}(\dot{\varepsilon}) \quad (19)$$

Finally, we arrive at the *EPFD* tangent relation:

$$E^{epf} - \frac{E^{epf}\frac{\partial F_{da}}{\partial\sigma} \otimes \frac{\partial F_{da}}{\partial\sigma}E^{epf}}{\left(\frac{\partial F_{da}}{\partial A_k^{da}}\right)^2 \frac{\partial^2 Y_f^{da}}{\partial(a_k^{da})^2} + \frac{\partial F_{da}}{\partial\sigma} : E^{ef} : \frac{\partial F_{da}}{\partial\sigma}}.$$

$$\dot{\sigma} = E^{epfd}(\dot{\varepsilon}) \quad (20)$$

3. Mapping to Hysterical Constitutive Law Based on EPFD

In this section, uniaxial constitutive law for plain or reinforced concrete subjected to earthquake loadings in both compression and tension is presented. Under real dynamic and earthquake loadings, quasi-brittle materials, like concrete, may experience complex loading processes involving not only full or partial loading- unloading- reloading processes in tension or compression spaces, but also mixed cycles involving compression and tension.

This uniaxial hysterical constitutive law was divided into compression envelope curve, tension envelope curve, compression unloading curves, tension unloading curves, compression reloading curves, tension reloading curves, partial unloading-reloading, and transition laws.

Most researchers commonly accept that the uniaxial monotonic stress-strain can approximate the envelope curve for concrete subjected to uniaxial hysterical compression [27, 30-33]. As shown in Figure (2), the envelope curves must verify some special conditions:

a) The initial slope at origin should be equal to the Yong modulus
b) This curve should present post peak coordinates correctly (maximum stress, and strain corresponding the maximum stress), ascending (hardening), and descending (softening) branches. In appendix (*II*), more explanation is provided about uniaxial constitutive law.

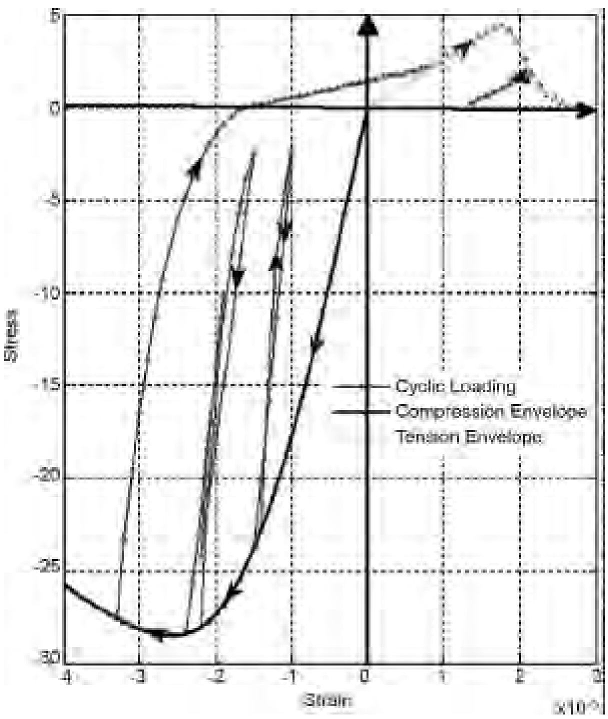

Figure 2. Crack-close model.

4. Reinforced Concrete Structure under Earthquake Motion

To further illustrate the capability of the proposed constitutive law, the simple shear wall is subjected to ground acceleration during several earthquake motions.

The equation of motion of a structure subjected to a single support seismic excitation $\ddot{u}_g(t)$, can be written as [34]:

$$[M]\{\ddot{u}\}+[C]\{\dot{u}\}+[K]\{u\}=-[M]\{r\}+\ddot{u}_g(t) \qquad (21)$$

in which the $n\times 1$ vector $\{u\}$ designates the relative displacements of the degrees of freedom; n is the number of degrees of freedom; $n\times 1$ the $\{r\}$ vector is the influence vector representing the displacement of each degree of freedom resulting from static application of a unit ground displacement; and the $n \times n$ matrices $[M]$, $[C]$ and $[K]$ represent the structural mass, damping and stiffness matrices, respectively.

The structural damping matrix $[C]$ is assumed to be proportional to the mass and stiffness matrices as [34]:

$$[C]=\propto_0[M]+\beta_0[K] \qquad (22)$$

where, $\propto_0$ is $\frac{2\xi_1\times\omega_1\times\omega_2}{\omega_1+\omega_2}$, β_0 is $\frac{2\xi_2}{\omega_1+\omega_2}$. In which $\propto_0$ and β_0 are the proportional coefficients; ω_1 and ω_2 are the structural modals frequencies of modes 1 and 2, respectively; and ξ_1 and ξ_2 are the structural damping ratios for modes 1 and 2.

The equation of motion of a nonlinear multi degree of freedom system subjected to a single seismic excitation $\ddot{u}_g(t)$ can be written as:

$$[M]\{\ddot{u}\}+[C]\{\dot{u}\}+[K_{nonlinear}]\{u\}=-[M]\{r\}+\ddot{u}_g(t) \qquad (23)$$

the $n\times 1$ vector $\{r\}$ is the influence vector representing the displacement of each degree of freedom resulting from static application of a unit ground displacement.

The state equations of the combined system can be written in the standard state-space form as follows:

$$\begin{cases}\{\dot{Z}\}=[A_1]\{Z\}+[B_1]\{eq\}\\ \{d\}=[C_1]\{Z\}\end{cases} \qquad (24)$$

in which the $[2n\times 1]$ state vector Z is $[\{u\}^T\{\dot{u}\}^T]^T$.

The state matrix $[A_1]$, input matrix $[B_1]$, output matrix $[C_1]$, vector $\{eq\}$ and output vector $\{d\}$ are, respectively, given by:

$$A_1 = \begin{bmatrix} 0_{(n+1)\times(n+1)} & 1_{(n+1)\times(n+1)} \\ -M^{-1}K & -M^{-1}C \end{bmatrix}$$

$$B_1 = \begin{bmatrix} 0_{(n+1)\times(n+1)} \\ I_{(n+1)\times(n+1)} \end{bmatrix} \quad (25)$$

$$\{eq\} = -\{r\}\ddot{u}_g(t)$$

$$C_1 = \begin{bmatrix} 0 & \dots & 1_m & 0 & \dots & 0 & \dots & 0 \\ 0 & \dots & 0 & 0 & 0 & 1_{m+n} & \dots & 0 \end{bmatrix}$$

$$\{d\} = [\{u_m\}^T \{\dot{u}_m\}^T]^T$$

in which O is a zero matrix and I is an identity matrix; 1_m indicates that the value of column n is unity; u_m and $\dot{u}_m$ are the displacement and velocity of the m^{th} degree of freedom, respectively. For solving this problem, the simulink of *MATLAB* (V.7.6.0) is used, see Figure (3).

To investigate the effectiveness of the nonlinear constitutive law for different disturbances, four different seismic motions are used in the numerical simulations. These ground acceleration records are: El Centro 1940, San Francisco 1957, Northridge 1994 and Kobe 1995 earthquakes. The absolute peak ground accelerations (*PGAs*) of these earthquake records are 0.29, 0.64, 0.112 and 0.44*g*, respectively, see Table (1) and Figures (4) and (5).

5. Numerical Study

5.1. Description of the CAMUS Experiment

In order to present a numerical model, the experimental results of a wall have been used. To achieve this goal, a 1/3 scaled model has been tested on the shaking table at *C.E.A.* [35]. The mock-up is shown in Figure (6).

The mock-up is loaded by horizontal acceleration parallel to the walls. The response spectra on Figure (6) shows the difference of these four kinds of earthquakes. The Rayleigh damping coefficients have been adjusted to impose a value of 1% on the first mode and 2% on the second mode. The material parameters are: E = 30000*MPa* for concrete with a maximum compressive strength of 35*MPa* and 3*MPa*

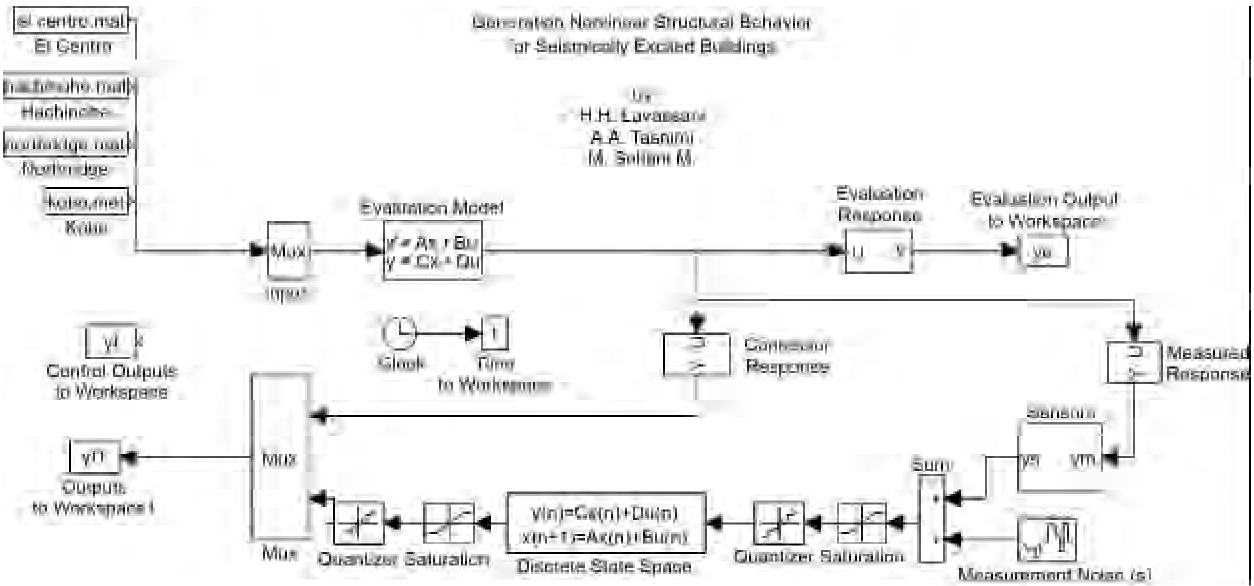

Figure 3. Generation of nonlinear structural system under seismically exciting motion.

Table 1. Earthquake ground motion information.

ID	Name	Location	PGA (g)	Duration	Ref.
F2	El Centro	Houston	0.29	39.09	NEIC[1]
F23	Kobe	Kobe	0.64	40.95	NEIC
F26	San Francisco	Golden Gate Park	0.11	39.59	NEIC
F25	Northridge	Beverly Hills	0.44	29.98	NEIC

1. National Earthquake Information Center

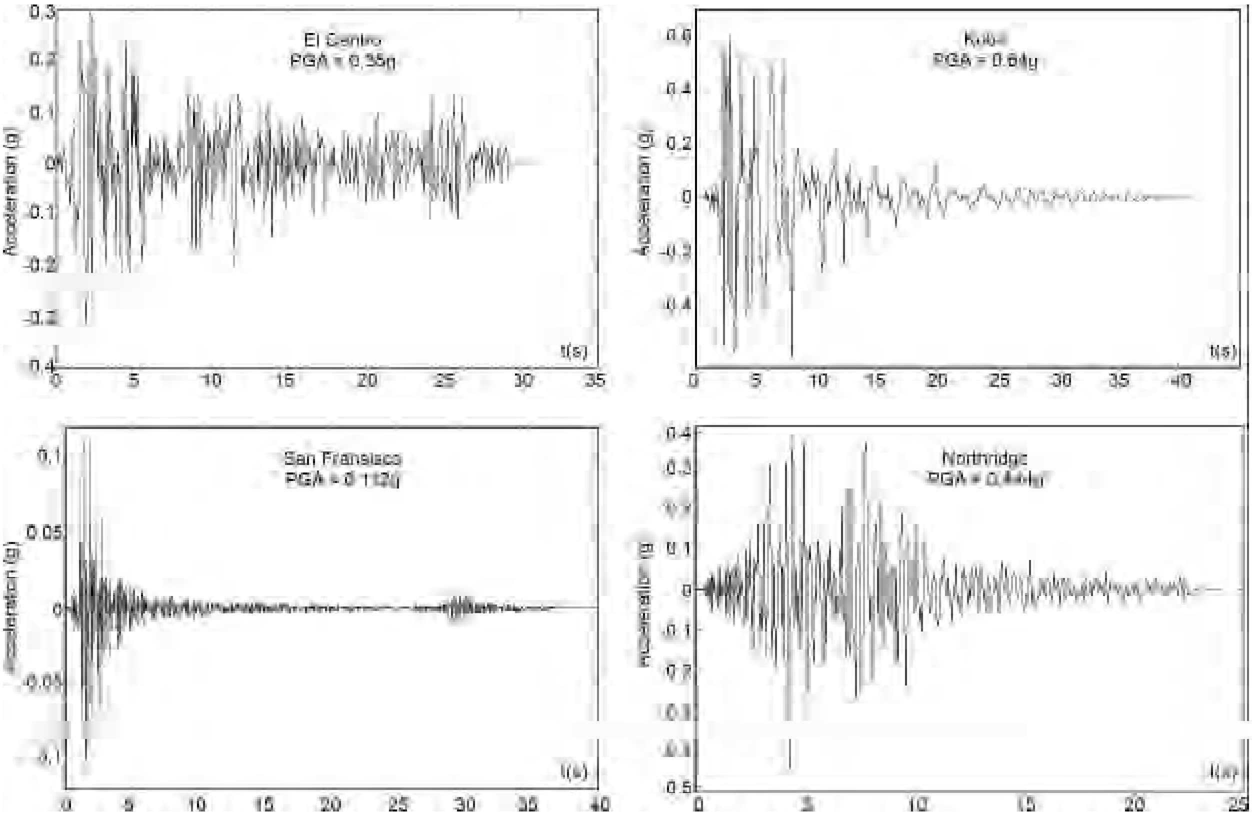

Figure 4. Time history of selected earthquakes.

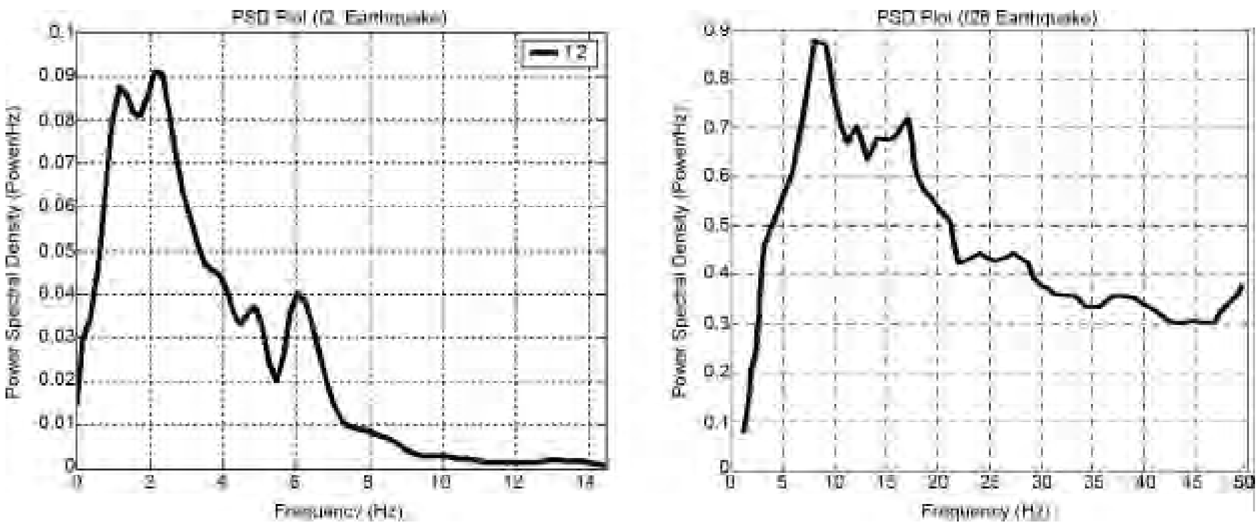

Figure 5. Spectrum of selected earthquakes (El Centro, San Francisco).

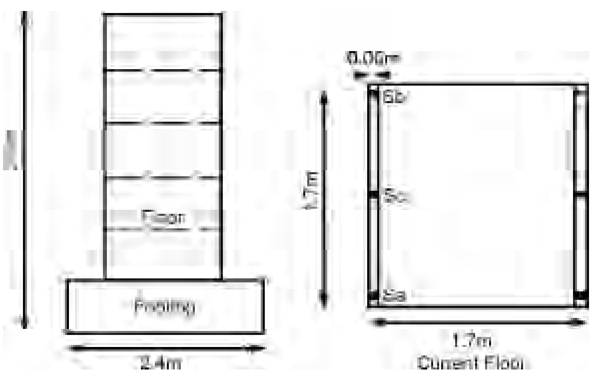

Figure 6. CAMUS mock up [36].

in tension. Concerning steel, E = 200000MPa, yield stress = 414MPa and the ultimate tensile strength is 480Mpa. Table (2) provides the ratio of steel reinforcement for each wall.

Figures (7) to (10) show the analytical response of the wall by the measured horizontal top displacement under selected earthquakes.

5.2. Constitutive Law of Concrete with Pre-Cracking Nonlinear Response

In this section, the uniaxial constitutive law of concrete with pre-cracking nonlinear response related to seismic engineering is evaluated. To achieve this, pre-cracking stress-strain relationship for one confined point in core of shear wall was presented in Figure (11).

Table 2. Steel reinforcement ratio for each wall (mm^2).

Various Levels	Sa, Sb	Sc
Level 5	15.9	78.4
Level 4	28.2	78.4
Level 3	94.4	110.2
Level 2	188.9	138
Level 1	289.4	138

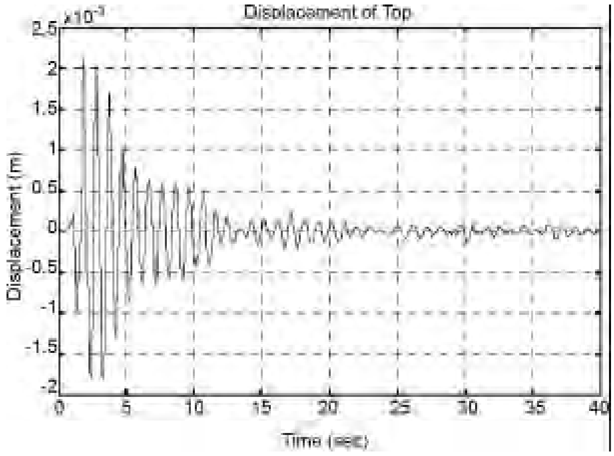

Figure 9. The displacement of top point of wall under San Francisco ground motion earthquake.

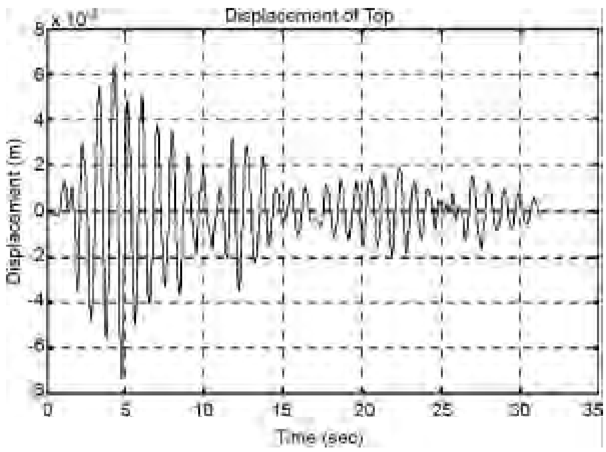

Figure 7. The displacement of top point of wall under El Centro ground motion earthquake.

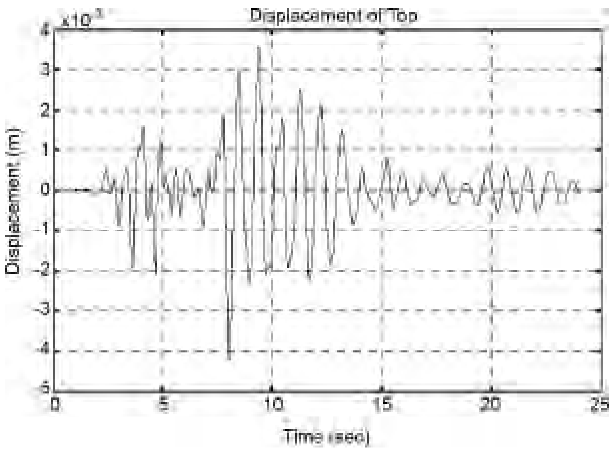

Figure 10. The displacement of top point of wall under Northridge ground motion earthquake.

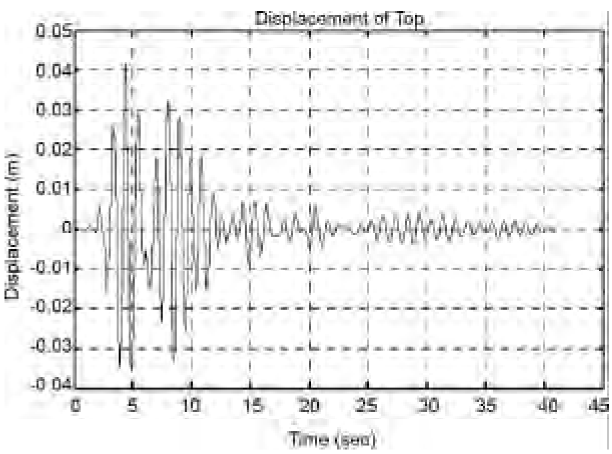

Figure 8. The displacement of top point of wall under Kobe ground motion earthquake.

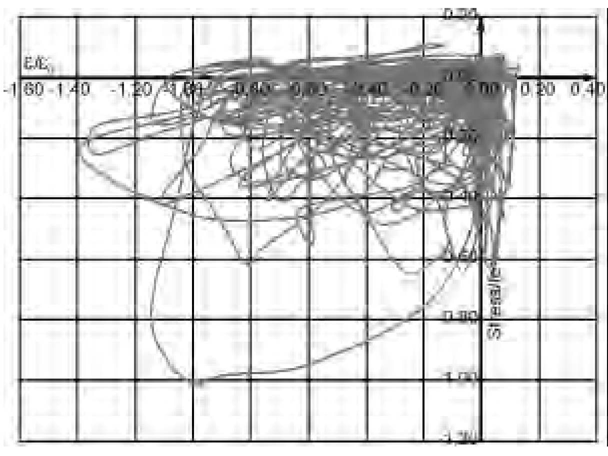

Figure 11. The stress-strain relationship of node 121 of shear wall under Northridge ground motion earthquake.

5.3. Affected Constitutive Law in Tension-Stiffening by the Bond Slip and Reinforcement Modeling

In this case study, a zero-thickness bond link is placed between reinforced and concrete to deal with bond-slip behavior. Because the main objective is to model the concrete material, a perfect bond between the concrete and the reinforcement is assumed. However, it is important to mention that the bond degradation of reinforcing bars is one of the weakest links of the seismic performance of reinforced concrete structures, and hence the bond-slip between the concrete and the reinforcement needs to be well modeled for further realistic nonlinear analysis. The widely used Giuffré-Menegotto-Pinto model [37] is employed in this study to represent the hysteretic stress-strain behavior of reinforcing steel. The tension envelope parameters of concrete near to reinforcement are dependent to bond slip and reinforcement modeling.

6. Conclusion

The aim of this work is principally the development of general nonlinear constitutive law for reinforced concrete. This constitutive law usually shows pressure-dependent behavior and non-associated flow rule, although the thermodynamics formulation described here could also find many other applications. Many theoretical laws for concrete have been proposed, involving a huge variety of methods, assumptions and procedures.

A combined 3D constitutive law based on thermodynamics for the simulation of the response of concrete subjected to earthquake loadings in both tension and compression has been offered, including an elasto-plastic-fracture model for concrete cracking based on the novel potential function and an elasto-plastic-damage model for concrete crushing based on the novel potential function. The hardening/ softening for the plasticity model was related to the plastic parameters, interacting with a nonlinear novel plastic potential function. Both models are globally formulated.

This law can reproduce the complex behavior of concrete under any history of uniaxial earthquake loading. Two sets of independent parameters, one for damage in compression and the other for fracture in tension, have been presented to model the descent of concrete under increasing loads. A one dimensional constitutive law based on thermodynamics is presented to model the cycles under earthquake loadings by considering its dependency on the damage and fracture parameters in concrete.

The behavior of this law was verified against several hysteretic loading histories and reasonable correlation with experimental results was generally observed. There are experimental results in the literature, for instance [27, 33], which could be used to improve the shear behavior of the model.

References

1. Bazant, Z.P. and Kim, S.S. (1979). “Nonlinear Creep of Concrete Adaptation and Flow”, *J. of Engineering Mechanic, ASCE*, **105**, 429-446.

2. Frantziskonis, G. and Desai, C.S. (1987). “Constitutive Model with Strain Softening”, *Int. J. Solids Struct*, **23**, 733-750.

3. Ju, J.W. (1989). “On Energy Based Coupled Elasto-Plastic Damage Theories: Constitutive Modelling and Computational Aspects”, *Int. J. Solids and Struct*, **25**, 803-833.

4. Ortiz, M.A. (1985). “Constitutive Theory for Inelastic Behaviour of Concrete”, Mech. Mater., **4**, 67-93.

5. Contrafatto, L. and Cuomo, M.A. (2006). “Frame Work of Elastic-Plastic Damaging Model for Concrete under Multiaxial Stress States”, *Int. J. of Plasticity*, **22**, 2272-2300.

6. Han-Chin, W. and Komarakul, N.A. (1999). “Constitutive Framework of Plastically Deformed Damaged Continuum and a Formulation Using the Endochronic Concept”, *Int. J. of Solids and Structures*, **25**, 4946-4976.

7. Resende, L. (1987). “A Damage Mechanics Constitutive Theory for the Inelastic Behavior of Concrete”, Computation Method Application Mechanics Engineering, **60**, 57-93.

8. Alexander, A. Lukyanov (2008). “Constitutive behavior of Anisotropic Material under Shock Loading”, *Int. J. of Plasticity*, **24**, 140-167.

9. Planas, J., Elices, M., Guinea, G.V., Gomez, F.J., Cend-on, and Arbilla, D.A.I. (2003). “Generalizations and Specializations of Cohesive Crack Models”, *Engineering Fracture Mechanics*, **70**, 1759-1776.

10. Hsieh, S.S., Ting, E.C., and Chen, W.F. (1979). “An Elastic-Fracture Model for Concrete”, *Proc.*

of the Third Engineering Mechanics Division Specialty Conference, ASCE, The University of Texas at Austin, Texas.

11. Ruiping, G. and Guangxin, L. (2008). "Elasto-Plastic Constitutive Model for Geotechnical Materials with Strain-Softening Behavior", *Computers & Geosciences*, **34**, 14-23.

12. Bazant, Z.P. (2002). "Concrete Fracture Models: Testing and Practice", *Engineering Fracture Mechanics*, **69**, 165-205.

13. Wilfried, B.K. and Rainer, P. (1998). "Elasto-Plastic Damage-Theories and Elasto-Plastic Fracturing Theories- a Comparison", *Computational Materials Science*, **13**, 117-131.

14. Wilfried, B.K. and Rainer P. (2004). "An Elasto-Plastic Damage Model for Reinforced Concrete with Minimum Number of Material Parameters", *Computers and Structures*, **82**, 1201-1215.

15. Xiaoya, T. and David, V. Ph. (2005). "A Simplified Isotropic Damage Model for Concrete Under Bi-Axial Stress States", *Cement & Concrete Composites*, **27**, 716-726.

16. Chen, W.F. and Han, D.J. (1988). "Plasticity for Structural Engineers", Springer-Verlag Inc, New York, USA.

17. Burlion, N., Gatuingt, F., Pijaudier-Cabot, G., and Daudeville, L. (2000). "Compaction and Tensile Damage in Concrete: Constitutive Modeling and Application to Dynamics", Computation Methods Application Mechanics Engineering, **183**, 291-308.

18. Rene de Borst. (2002). "Fracture in Quasi-Brittle Materials: A Review of Continuum Damage-Based Approaches", *Engineering Fracture Mechanics*, **69**, 95-112.

19. Widmann, R. (1990). "Fracture Mechanics and Its Limits of Application in the Field of Dam Construction", *Engineering Fracture Mechanics*, **135**(1-3), 532-539.

20. Zhijun, Zh. and Ansari, F. (2006). "Fracture Mechanics of Air-Entrained Concrete Subjected to Compression", Engineering Fracture Mechanics, **73**, 1913-1924.

21. Ricardo, A., Einsfeld, M., and Velasco, S.L. (2006). "Fracture Parameters for High-Performance Concrete", *Cement & Concrete Composites*, **36**, 576-583.

22. Chang, C.S., Wang, T.K., Sluys, L.J., and Van Mier, J.G.M. (2002). "Fracture Modeling Using a Micro-Structural Mechanics Approach--I, Theory and Formulation", *Engineering Fracture Mechanics*, **69**, 1941-1958.

23. Ludovic, J., Antonio, H., and Gilles Pijaudier-Cabot, Sh. (2006). "An Elastic Plastic Damage Formulation for Concrete: Application to Elementary Tests and Comparison with an Isotropic Damage Model", *Comput. Methods Appl. Mech. Engineering*, **195**, 7077-7092.

24. Popovics, S. (1970). "A Review of Stress-Strain Relationship of Concrete", *ACI. Journal*, **67**(3).

25. Popovics, S. (1973). "A Numerical Approach to the Complete Stress-Strain Curve of Concrete", Cement and Concrete Research, **3**(5), 583-599.

26. Collins, M.P. and Porasz, A. (1989). "Shear Design of High Strength Concrete", CEB Bulletin d' Information, **193**, 77-83.

27. Tasnimi, A.A. (2002). "A Nonlinear Mathematical Model for Stress-Strain Relationship of Plain and Reinforced Concrete", Research Report of Sabbatical Leave at University, Tokyo.

28. Houlsby, G.T. and Puzrin, A.M. (2000). "A Thermo Mechanical Framework for Constitutive Models for Rate-Independent Dissipative Materials", *Int. J. of Plasticity*, **16**, 1017-1047.

29. Hill, R. (1968). "On Constitutive Inequalities for Simple Materials--I", *J. Mechanics and Physics Solids*, **16**, 229-242.

30. Karsan, I.D. and Jirsa, J.O. (1969). "Behavior of Concrete under Compressive Loadings", *J. Structure Div. ASCE*, **95**(ST12), 2543-63.

31. Yankelevsky, D.Z. and Reinhardt, H.W. (1987). "Model for Cyclic Compressive Behavior of Concrete", *Journal Structure Engineering, ASCE,* **113**(2), 228-40.

32. Bahn, B.Y. and Hsu, C.T. (1998). "Stress-Strain Behavior of Concrete under Cyclic Loading", *ACI Mat. J.*, **95**(2), 178-93.

33. Tasnimi, A.A. (2004). "Mathematical Model for

Complete Stress-Strain Curve Prediction of Normal, Light-Weight and High-Strength Concrete", Magazine of Concrete Research, **56**(1), 23-34.

34. Clough, R.W. and Penzien, J. (1993). "Dynamics of Structures", 2nd Edition, Mc Graw-Hill, New York, USA.

35. Armstrong, P.J. and Frederick, C.O. (1966). "A Mathematical Representation of the Multiaxial Bauschinger Effect", G.E.G.B. Report RD/B/N 731.

36. Mansour, M. and Hsu, T.T.C. (2005). "Behavior of Reinforced Concrete Elements under Cyclic Shear II: Theoretical Model", *Journal Structure Engineering, ASCE*, **131**(1), 54-65.

37. Menegotto, M. and Pinto, P.E. (1973). "Method of Analysis for Cyclically Loaded Reinforced Concrete Plane Frames Including Changes in Geometry and Non-Elastic Behavior of Elements under Combined Normal Force and Bending", *In: Proceedings of IABSE Symposium on Resistance and Ultimate Deformability of Structures Acted on by Well Defined Repeated Loads*, Lisbon.

38. Palermo, D. and Vecchio, J. (2003). "Compression Field Modeling of Reinforced Concrete Subjected to Reversed Loading: Formulation", *ACI Structure Journal*, **100**(5), 616-25.

39. Jos´e Fernando Sima, Pere Roca, and Climent, M. (2008). "Cyclic Constitutive Model for Concrete", *Engineering Structures*, **30**, 695-706.

Appendix I (Potential Approach)

In order to obtain a nonlinear theory, let us assume that there exists a function F such as:

$$\dot{a}_\kappa = \dot{\lambda}\frac{\partial F}{\partial A_\kappa};\ \dot{\lambda} \geq 0 \tag{A1-1}$$

The function F is called the *EPFD* mechanical dissipation potential and depends on the *EPFD* conjugated thermodynamics forces A_κ, but it may as well depend on some other material parameters Z_p. Returning to the *EPFD* mechanical dissipation potential gives:

$$d^f_{mech} = \dot{\lambda} A_\kappa \frac{\partial F(A_\kappa, Z_p)}{\partial A_\kappa} \geq 0 \tag{A1-2}$$

The *EPFD* mechanical dissipation potential in a slightly more convenient form is divided to three terms:

$$F = F_{pl} + F_{da} + F_{fr} \tag{A1-3}$$

According to the *EPFD* mechanical dissipation potential terms, the *EPFD* conjugated thermodynamics force sets A_κ and *EPFD* flux sets $\dot{a}_\kappa$ must be divided into subsets plastic, damage and fracture conjugated thermodynamics forces $A_\kappa = \{\{A_k^{pl}\}\{A_k^{da}\}\{A_k^{fr}\}\}$, and subsets plastic, damage and fracture fluxes $\dot{a}_\kappa = \{\{\dot{a}_k^{pl}\}\{\dot{a}_k^{da}\}\{\dot{a}_k^{fr}\}\}$.

The plastic potential functions are constituted by using the unified coordinates in the Haigh-Westergaard stress state which are based on the tensor invariant variables [16]. The analysis will be restricted to isotropic behavior. Therefore the Haigh-Westergaard representation of the yield locus is employed, and the corresponding three unified coordinates ζ, ρ and θ are defined as [29]:

$$\zeta = I_1 \tag{A1-4}$$

$$\theta = \frac{1}{3} Arccos\left(\frac{3\sqrt{3}}{2}\frac{J_3}{\sqrt{J_2^3}}\right) \tag{A1-5}$$

$$\rho = \sqrt{J_2} \tag{A1-6}$$

Where (I_1, J_2, J_3) are the first invariant variables of the plastic conjugated thermodynamics force tensor $\frac{\partial Y_f}{\partial \varepsilon_{ij}^{pl}}$, second, and third invariant variables of the plastic conjugated thermodynamics forces deviatory tensor. The plastic potential function can be written as:

$$F_{pl} = F_{pl1}(I_1) + F_{pl2}(J_2, J_3) \tag{A1-7}$$

where plastic potential function F_{pl} includes two functions F_{pl1} and F_{pl2}:

$$F_{pl1} = -Z D_i \sqrt{(\varphi^2 + Z B_i \varphi)(1 - \varphi^{ZC_i})} \tag{A1-8}$$

Where, $\varphi = Z A_i I_1 - \sqrt{3}\sigma_s$,

$$F_{pl2} = \sqrt{J_2} cos(\frac{1}{3} cos^{-1}(Z a_j \frac{J_3}{\sqrt{J_2^3}}) - Z b_j) \tag{A1-9}$$

Where, $0 \leq Z a_j \leq \frac{3\sqrt{3}}{2}$ and $0 \leq Z b_j \leq \frac{\pi}{2}$.

Appendix II (Uniaxial Constitutive Law)

A2.1. Compression Envelope Curve

In this paper, the compression envelope curve is proposed by Tasnimi for a complete Elasto-plastic damage constitutive law for plane and reinforced concrete [33]. This envelope equation is defined by a set of parameters that can be obtained in a uniaxial test, such as initial tangent modulus of elasticity, secant modulus corresponding compression strength, stress and strain at turning point, strain corresponding to the peak stress of envelope curve, and density of concrete.

The compression envelope equation that can be proposed for concrete in this section can be written as, see Figure (A.1):

$$\frac{\bar{\sigma}^-}{f_c} = \frac{n^{pq}}{\left[\left(\frac{\varepsilon^-}{\varepsilon_0}\right)^{n^{pq}} + n^{pq} - 1\right]} \frac{\varepsilon^-}{\varepsilon_0} \qquad \text{(A2-1)}$$

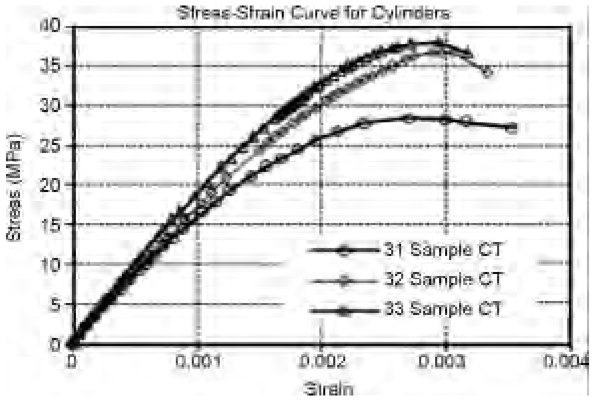

Figure A.1. Compression envelope curve and experimental results.

For the compression envelope equation, the value of n^{pq} is $\varepsilon_0 E_{tang}^{itm}(\varepsilon_0 E_{tang}^{itm} - f_c)^{-1}$.

For ascending portion, p is equal to three and q is equal to one. Therefore, n is known if value of concrete compression strength, strain corresponding to the peak stress, and initial tangent modulus of elasticity are known. For descending envelope region, if the uniaxial constitutive law of the structural elements contains a turning point on its descending section of the uniaxial envelope, the following are obtained:

$$n^{pq} = ln\left(\frac{\varepsilon_{tp}^-}{\varepsilon_0} + 1\right) \times \left(ln\left(\frac{\varepsilon_{tp}^-}{\varepsilon_0}\right)\right)^{-1} \qquad \text{(A2-2)}$$

The envelope equation can be rewritten as:

$$\frac{\sigma^-}{f_c} = \left(1 - \alpha_{da}^-\right) \frac{\varepsilon^-}{\varepsilon_0} \qquad \text{(A2-3)}$$

The damage parameter α_{da}^- is $((\frac{\varepsilon^-}{\varepsilon_0})^{n^{pq}} - 1) \times \left[(\frac{\varepsilon^-}{\varepsilon_0})^{n^{pq}} + n^{pq} - 1\right]^{-1}$.

A2.2. Tension Envelope Curve

On the other hand, this envelope curve that used to compression area, is applied for a complete Elasto-plastic-fracture constitutive law for plane and reinforced concrete in tension state [33]. The tension envelope equation is defined by the other set of parameters that can be obtained in a uniaxial tension test, such as initial tangent modulus of elasticity, secant modulus corresponding tension strength, stress and strain at tension turning point, strain corresponding to the peak tension stress of envelope curve, and density of concrete.

The tension envelope equation that is proposed for concrete by Tasnimi [33] can be written as, see Figure (A.2):

$$\frac{\sigma^+}{f_t} = \frac{m^{pq}}{\left[\left(\frac{\varepsilon^+}{\varepsilon_t}\right)^{m^{pq}} + m^{pq} - 1\right]} \frac{\varepsilon^+}{\varepsilon_t} \qquad \text{(A2-4)}$$

For the tension envelope equation, the value of m^{pq} is $(1 - f_t \varepsilon_t^{-1} E_{tang}^{itm\ -1})$. For linear tension ascending portion m equals zero. For descending tension envelope region, if the uniaxial constitutive law of the structural elements contains a turning point on its descending section of the uniaxial envelope, the following are obtained:

$$m^{pq} = ln\left(\frac{\varepsilon_{tp}^+}{\varepsilon_t} + 1\right) \times \left(ln\left(\frac{\varepsilon_{tp}^+}{\varepsilon_t}\right)\right)^{-1} \qquad \text{(A2-5)}$$

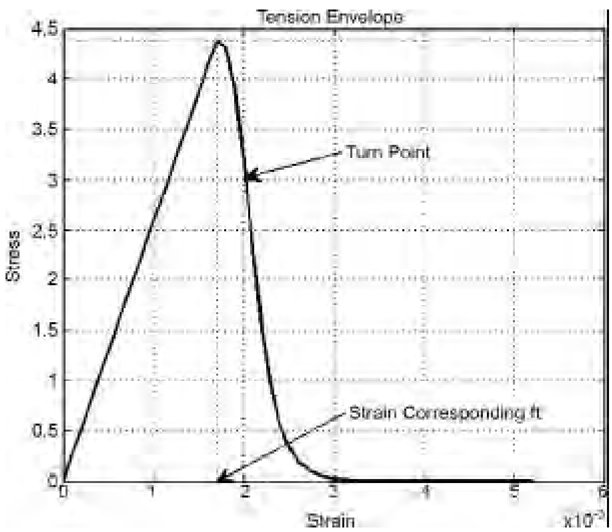

Figure A.2. Tension envelope curve.

The envelope equation can be rewritten as, see Figure (A.3):

$$\frac{\sigma^+}{f_t} = \left(1-\alpha_{fr}^+\right)\frac{\varepsilon^+}{\varepsilon_t} \tag{A2-6}$$

the fracture parameter α_{fr}^+ is:

$$((\frac{\varepsilon^+}{\varepsilon_t})^{m^{pq}}-1)\left[(\frac{\varepsilon^+}{\varepsilon_t})^{m^{pq}}+m^{pq}-1\right]^{-1}.$$

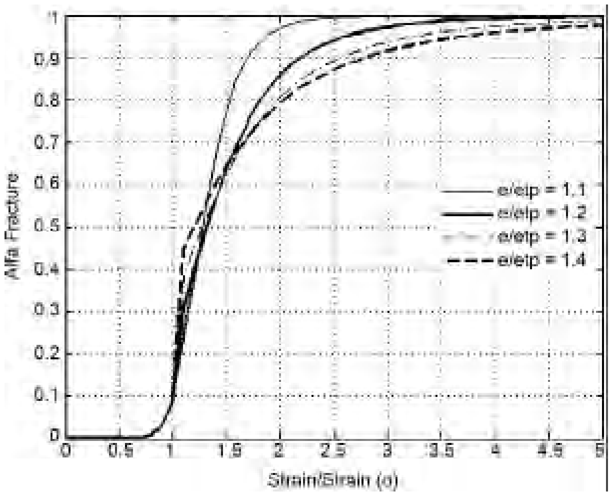

Figure A.3. Fracture parameter.

A2.3. *Unloading and Reloading Constitutive Law in Compression*

In many literature, the behavior of plain or reinforced concrete, when a specimen loaded up to certain stress and then unloaded to a base stress level, has shown, under a typical hysterical loading [31-33]. In this action, the compression unloading constitutive law contained maximum stiffness and started from unload point. This is illustrated in Figure (A.4).

The condition of the unloading and reloading compression laws depends on the amount of non recoverable damage in the compression region. Many models consider the unloading strain as the parameter that defines the unloading and reloading path and determines the degree of damage caused by the cycling [30-35, 37-38]. Some kind of equations have been used to reproduce the unloading equation also, like the Ramberg-Osgood equation used by [38], the power type used by [36] or the multi linear curve proposed by [39]. On the other hand, [37] present power type unloading and linear reloading. In all above researches, the equations of envelope, unloading, and reloading are not unique. In this paper, those equations are based on general constitutive law, and are integrated. This novel uniaxial reloading constitutive law proposed for the unloading curve includes the mean features of the unloading equations obtained experimentally, such as, see Figure (A.5):

- The curvature parameter of the unloading equation,
- The initial unloading stiffness,
- The final unloading stiffness,
- The unloading strain and plastic strain.

The relationships of compression reloading curve can be expressed:

$$\frac{\sigma^-}{\sigma_{re}} = \left(1-\alpha_{r,da}^-\right)\left(\frac{\varepsilon_{re}}{\sigma_{re}}E_{re}^-\right)\frac{\varepsilon^- - \varepsilon_{pl}^{i-}}{\varepsilon_{re}} \tag{A2-7}$$

The damage parameter of reloading $\alpha_{r,da}^-$ is the function of (ε^-).

A2.4. *Partial Unloading and Reloading Constitutive Law in Compression*

In contrast to other relationships, which were presented in the literature, this stress-strain relation-

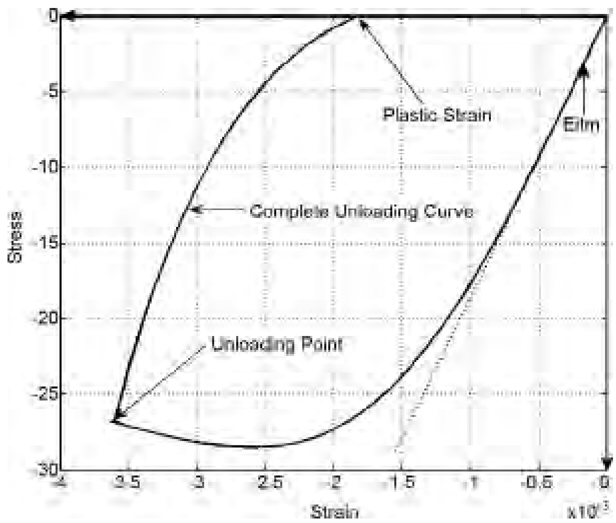

Figure A.4. Curve of complete unloading.

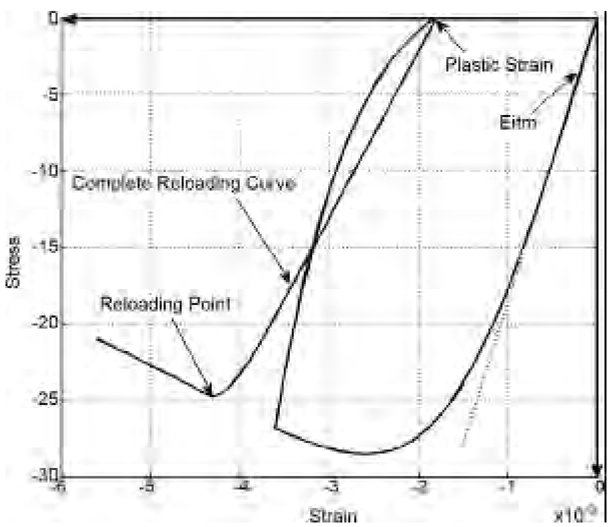

Figure A.5. Curve of complete reloading.

ship considers the behavior of plain or reinforced concrete in the case of partial unloading and reloading. The equation proposed herein for the general case of partial unloading and reloading cycles are based on the same test data, see Figures (A.6) and (A.7). The relationships of partial compression reloading curve can be expressed:

$$\sigma^{-} - \sigma_{un}^{i-} = (1 - \sigma_{r,da}^{p-})\, E_{re}^{-} \frac{\varepsilon^{-} - \varepsilon_{un}^{i-}}{\varepsilon_{re} - \varepsilon_{un}^{i-}} \qquad \text{(A2-8)}$$

The partial damage parameter of reloading $\alpha_{r,da}^{p-}$ is function of (ε^{-}).

As suggested by experimental result, when a partial unloading occurs following by reloading to meet the envelope curve, the reloading path can be modeled by the same equation as envelope equations.

A2.5. *Unloading and Reloading Constitutive Law in Tension*

Hysterical behavior is modeled by the same tension envelope. An equation same as tension envelope equation is used for the reloading branch:

$$\frac{\sigma^{+}}{f_t} = \frac{(m^{pq} - 1)\,(\varepsilon_{un}^{+})^{-1.05}}{[(\frac{\varepsilon_{un}^{+}}{\varepsilon_t})^{m^{pq}} + m^{pq} - 1]} \frac{\varepsilon_t^{2.05}}{f_t} E_{tan}^{itm} \frac{\varepsilon^{+}}{\varepsilon_t} \qquad \text{(A2-9)}$$

So, a linear equation is used for the unloading branch. Based on the experimental data from [31], the following criterion is proposed to account for the stiffness deterioration:

$$\frac{\sigma^{+} - \sigma_{un}^{+}}{f_t} = \frac{\varepsilon_t^{2.05}}{f_t (\varepsilon_{un}^{+})^{1.05}} E_{tan}^{itm} \frac{\varepsilon^{+} - \varepsilon_{un}^{+}}{\varepsilon_t} \qquad \text{(A2-10)}$$

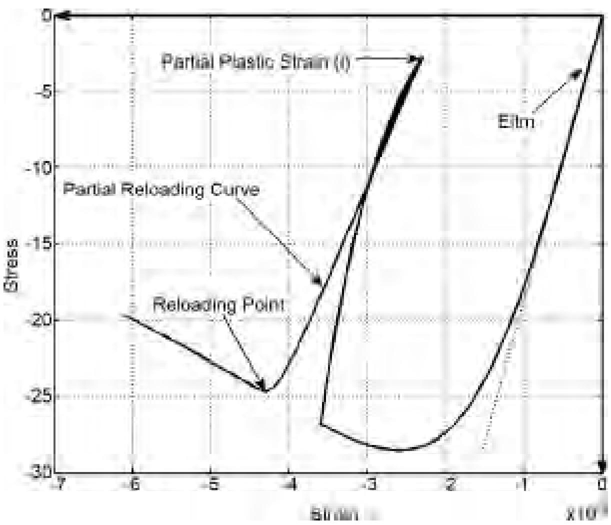

Figure A.6. Curve of partial reloading.

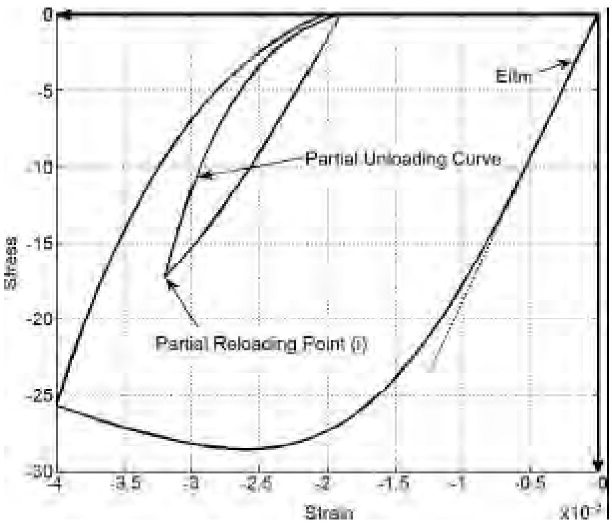

Figure A.7. Curve of partial unloading.